The Fluid Dynamics of Taylor Cones

Juan Fernández de la Mora

Department of Mechanical Engineering, Yale University, New Haven, Connecticut 06520-8286; email: juan.delamora@yale.edu

Annu. Rev. Fluid Mech. 2007. 39:217–43

The *Annual Review of Fluid Mechanics* is online at fluid.annualreviews.org

This article's doi:
10.1146/annurev.fluid.39.050905.110159

0066-4189/07/0115-0217$20.00

Key Words

electrospray, cone-jet, charged interface, charged drop, Coulomb fission, space charge

Abstract

The formation of cone-jets in charged liquids with electrical conductivities larger than 10^{-4} S/m is reviewed for steady supported menisci and transient Coulomb fissions in charged drops. Taylor's hydrostatic model does not apply strictly, but it forms the basis for subsequent developments. The jet structure is critically dependent on the model used for charge transport, which has been based mostly on a constant conductivity assumption. Saville's (1997) more general model predicts the formation of rarefaction fronts with wide space charge–dominated regions near the liquid surface, which apparently do arise in polar liquids near the minimum flow rate. Known approximate scaling laws for the jet break down at electrical conductivities of about 1 S/m due to ion evaporation from the meniscus. In molten salts and liquid metals a regime of purely ionic emissions exists without drop or jet formation.

1. INTRODUCTION

Electrospray (ES): a cloud of charged drops formed from a Taylor cone

When the interface between an electrically conducting liquid and an insulator [often air or a vacuum, but sometimes a dielectric liquid (Barrero et al. 2004)] is charged electrically beyond a certain critical level, it becomes unstable and evolves from a generally rounded shape to another including one or several remarkably stable conical features called Taylor cones. The initial loss of stability can be easily predicted by linear analysis of an inviscid, infinitely conducting liquid for a planar surface under gravity charged by a uniform external field (Frenkiel instability) (Landau & Lifshitz 1960, Taylor 1965), as well as for a charged drop in a field-free environment (Rayleigh 1882, 1945). Once the instability arises, new interfaces with conical features often form, and are the subject of this review. **Figure 1** shows several examples of stationary and transient Taylor cones.

Taylor cones may be stationary, but they are never static features. Their apices are always the source of emission of charged particles under a rich range of regimes, many of which have been classified by Cloupeau & Prunet-Foch (1989, 1990, 1994) and Cloupeau (1994). They all remain incompletely and even poorly understood, but a considerable literature has accumulated on the simplest and apparently most useful one, the cone-jet. In this regime, a steady jet issues continuously from the cone apex, eventually breaking into a spray of charged drops, or electrospray (ES). Most of our discussion relates to this steady regime, which is not only the best known, but also the simplest to analyze, and by far the most useful in practice. We further slant the review toward the limit of high electrical conductivity (0.001–1 S/m) of the

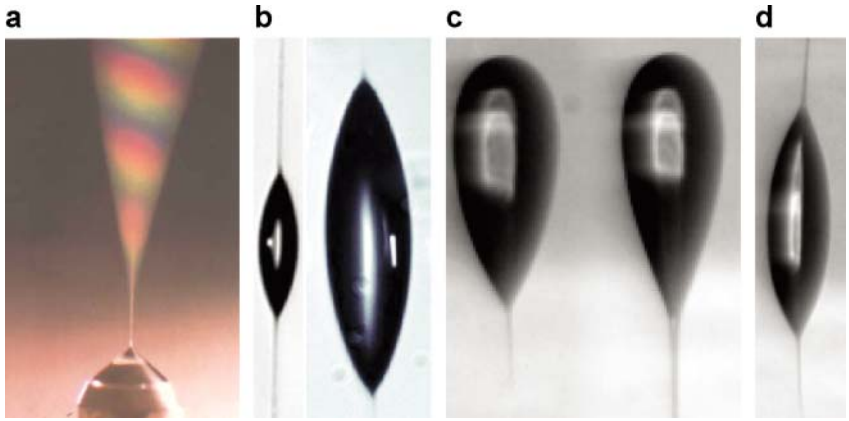

Figure 1

Examples of stationary and transient Taylor cones. (*a*) Steady cone-jet supported on a charged capillary needle (figure 1*b* of Pantano et al. 1994). (*b*) Symmetric explosion of a drop of ethylene glycol 24 μm in diameter charged at the Rayleigh limit with no external field (from figure 4 of Achtzehn et al. 2005). (*c*) Asymmetric explosion of 225 μm methanol drops charged at 13% of the Rayleigh limit in an external field of 2.21 10^6 V/m (from figure 8*b* of Grimm & Beauchamp 2005). (*d*) Symmetric explosion of an uncharged methanol drop 225 μm in diameter in an external field of 2.18 10^6 V/m (from figure 5*a* of Grimm & Beauchamp 2005). All reprinted with permission.

liquid, where the jet radius is typically smaller than 1 μm, and the large disparity of scales between jet width and meniscus size enables a division of the problem into two regions. An outer domain (the cone), which is effectively hydrostatic [in the restricted sense that the recirculating flows that sometimes form (Barrero et al. 1998, Cherney 1999, Hayati et al. 1986) are slow and have little influence on jet formation], in which the liquid behaves as infinitely conducting, and an inner region, which is dynamic and where a very fine jet carrying a finite current and flow rate forms. Taylor cones of highly conducting liquids offer the only known scheme to produce submicrometer and nanometer jets (down to a diameter of about 10 nm). On the other hand, the low conductivity limit is of relatively modest theoretical interest, as the jet becomes thick and poorly differentiated from the meniscus. The cone and the jet then cease to be singular, and a number of controlling parameters that play almost no role at high conductivity affect the behavior in a still unknown fashion. Low liquid conductivities are also of limited practical interest because many alternative and generally much simpler schemes exist to produce thick jets.

Although the vast electrospray mass spectrometry (ESMS) literature (more than 1500 published articles/year) lies almost entirely outside fluid dynamics, the associated technique to ionize large biomolecules (Fenn et al. 1989) has had a formidable impact on mass spectrometry, and through it on biology, chemistry, and medicine. Still, the physical basis behind ESMS, for which John B. Fenn received the 2002 Nobel Prize in chemistry, is fundamentally fluid dynamical, and its initial development followed directly from Fenn's earlier interests in hypersonic free jets (Fenn 1996).

In this review, we first consider the idealization of static pointed liquid tips, which does not hold rigorously, but whose simplicity has enabled considerable progress in the field. Section 3 considers the effect of the finite conductivity of the liquid, the main factor fixing the width of the jet. It has been modeled mostly via a constant conductivity (ohmic model), although a more general model (Saville 1997) is also discussed. We then review what is known, primarily from experimentation, about Taylor cone-jets at high electrical conductivity, either supported on stationary menisci (Section 4) or drops (Section 5). Finally, Section 6 considers the extreme limit when the electrical conductivity reaches values of 1 S/m, at which the resulting jet diameters of about 10 nm give rise to electric fields in the range of 1 V/nm and evaporation of ions.

ESMS: electrospray mass spectrometry

Space charge: net charge resulting from imbalance between the density of positive and negative charges

2. THE STATIC STRUCTURE OF THE TAYLOR CONE

Let us start by ignoring the dynamic region of the cone forming near its apex and examine the outer problem, which is hydrostatic. Although much simpler than the real problem, the solution to the static problem has many features of real cone-jets, as it fixes onset voltages (relevant to certain pieces of the stability boundary of the cone-jet), illuminates certain observed features of hysteresis phenomena, and provides analytical features of the far field that affect the dynamic properties of the jet region. Taylor (1964) described the hydrostatic structure of what we shall call the pure Taylor cone, in which a balance (Equation 1) between capillary and electrostatic stresses is satisfied exactly on the surface of an equipotential cone. In the absence of space charge in the insulating medium, the electrical potential ϕ is given in Equation 2 in spherical

coordinates (r, θ) in terms of the Legendre function of order 1/2 (regular at θ = 0):

$$\gamma \nabla \cdot \mathrm{n} - {}^1\!/_2\, \varepsilon_o (\nabla \phi)^2 = \Delta p; \quad \phi = a_o\, r^{1/2}\, P_{1/2}(\cos\theta), \tag{1,2}$$

$$a_o^{-2} = {}^1\!/_2\, \gamma^{-1} \varepsilon_o P'^{2}_{1/2}(\cos\alpha_T) \tan\alpha_T = 0.552(\varepsilon_o/\gamma)^{1/2}; \quad P_{1/2}(\cos\alpha_T) = 0, \tag{3,4}$$

where γ is the interfacial tension between the conductor and the insulator, **n** is the normal to the surface directed toward the insulating medium, ∇.n is the curvature, ε_o is the electric permittivity of the insulator, and Δp is the pressure in the conducting liquid above that in the insulator. Substituting Equation 2 in Equation 1 and computing ∇.n for a cone of angle α_T fixes the constant a_o as given in Equation 3, also yielding $\Delta p = 0$. The cone angle α_T ($180^\circ - 49.29^\circ$) is fixed by Equation 4 after demanding that the surface be equipotential. This simple solution has greatly clarified the problem, but there are missing elements. First, Equation 2 corresponds to a special case when Δp is exactly zero, whereas other values are possible. In particular, the parametric range where the Taylor cone can be stabilized and the appearance of multiple solutions and hysteresis seem to be intimately tied to the finite range of possible values of Δp. Rather than describing one Taylor cone structure, one should strive to describe a family of them. Second, Equation 2 is valid only locally, because the corresponding ϕ is singular on the $\theta = \pi$ semiaxis and grows without bound in all directions as the distance r to the apex increases.

2.1. Stability Boundaries and Hysteresis

The role of Δp in fixing the range of voltages and meniscus shapes within which a Taylor cone can be stabilized is clearly seen in the study of Pantano et al. (1994). For a charged meniscus resting on the tip of a capillary tube, the authors search numerically for hydrostatic solutions with a conical tip, and find them only within a finite range of voltages, with a different geometry associated to each voltage. The meniscus shapes include an almost conical example at $\Delta p = 0$, separating a family of short pointed menisci curved away from the axis ($\Delta p < 0$, as in **Figure 1*a***) from another family of long acorn-shaped pointed menisci curved toward the axis ($\Delta p > 0$, as in **Figure 1*b***). Most ES studies have controlled the Taylor cone through the voltage V and the flow rate Q of liquid injected into the meniscus. However, Δp and V can also be controlled directly (Smith 1986, Zeleny 1915). In addition to providing hydrostatic information, this approach is often experimentally simpler than the alternative of controlling minute flow rates.

The existence of multiple solutions and associated hysteretic phenomena is well known. First consider the meniscus of **Figure 1*a***, where the conducting liquid is supported at the exit of a capillary tube. As the tube voltage V is increased with respect to surrounding electrodes, a first critical voltage V_1 is encountered at the point where the previously rounded meniscus becomes conical. However, when the voltage is subsequently slowly reduced, the meniscus remains conical down to a second voltage $V_o < V_1$. Therefore, at least two stable shapes exist in the range $V_o < V < V_1$, one rounded, the other conical. The pointed family extends above V_1, and the rounded family below V_o. The existence of this finite range of voltages at which pointed tips

are observed is compatible with the preceding hydrostatic considerations because the meniscus volume is free to vary with the imposed voltage.

Now consider the often-studied case of a charged drop with a fixed charge q_1 and a radius R slowly decreasing due to solvent evaporation. There is similarly a critical radius R_1, at which the spherical shape loses stability (the Rayleigh limit, Rayleigh 1882), at which

$$q_1 = q_R(R) = 8\pi(\varepsilon_o \gamma R^3)^{1/2}, \tag{5}$$

and a pointed drop with one or two Taylor cones and associated jets forms (**Figure 1*b***). This leads to the loss of very little mass but substantial charge (up to 50%) in highly conductive drops in (Richardson et al. 1989). The emission then proceeds to a final charge $q_o < q_1$, at which point the drop becomes spherical again with a final radius R_2 indistinguishable from R_1. Because all the charge is lost through the Taylor cones, the pointed drop remains stable at a fixed volume through the whole range of charges $q_o < q < q_1$. But a spherical drop is also stable over that full range; hence, there are at least two stable drop shapes over that range. In fact, the branch of pointed shapes probably extends to a charge level $q_2/q_1 > 1$, although an experimental study of them would be challenging. Unlike the supported menisci just discussed, however, this finite range of pointed drops cannot represent hydrostatic solutions of the problem. Indeed, because the volume is now fixed, only one (or a few) isolated hydrostatic solution(s) can exist for a special value q^* of the charge. We argue below that space charge associated to the spray (or the jet) ejected by the cone apex can stabilize a pointed drop at a charge larger than the critical value q^* (computed in the absence of space charge). This mechanism, however, does not stabilize a pointed drop charged below q^*, so the real conical meniscus must lose stability and turn spherical precisely at q^*. We therefore conclude that the experimentally observed value of q_o ($\sim q_1/2$ based on the data of Richardson et al. 1989 and Li et al. 2005) must be relatively close to the theoretically calculable value q^*.

2.2. Curved Taylor Cone

We seek a generalization of Equation 2 that gives a Taylor cone with a finite pressure jump Δp. Below is a preliminary attempt to do so, leaving out possible eigenfunctions noted by F. Higuera (private communication, 2006). For an axisymmetric pointed tip with its apex located at $r = 0$, the following expansion in half-integer powers of the rescaled polar coordinate $\rho = a_1 r$ satisfies Laplace's equation:

$$\begin{aligned}\phi(\rho, \theta) = a_0 r^{1/2}\{&P_{1/2}(\cos\theta) + \alpha_1 \rho P_{3/2}(\cos\theta) + \alpha_2 \rho^2 P_{5/2}(\cos\theta) \\ &+ \cdots + \alpha_n \rho^n P_{n+1/2}(\cos\theta) + \cdots\}, \rho = r\, a_1.\end{aligned} \tag{6,7}$$

Postulating a perturbed Taylor cone geometry of the form

$$\theta(r) = \alpha_T + \beta_1 \rho + \beta_2 \rho^2 + \beta_3 \rho^3 + \beta_4 \rho^4 + \cdots, \tag{8}$$

the condition that the surface be equipotential, and Equation 1 stating that the surface is also in mechanical equilibrium, fix the pressure jump as well as the values of the

Table 1 Initial a_n and s_n coefficients calculated for the series (6) and (8)

n	1	2	3	4	5	6	7	8	9
α_n	1	1.34872	2.15378	3.28424	4.82025	6.71530	8.37544	8.12630	1.96622
β_n	−0.5053	0.2718	−0.2090	−0.2114	0.27853	0.40655	−0.5829	0.82082	−1.1725

expansion coefficients, as detailed in **Table 1**.

$$\Delta p/\gamma = -0.524826\ a_1 \tag{9}$$

It is interesting to note that, to all orders, the single parameter a_1 completely determines the potential and the meniscus shape. Because a_1 is uniquely related to the dimensionless pressure jump Δp, we confirm the anticipated notion that Δp affects the tip shape. In reality, except for a trivial change of scale by a factor a_1, there are only three Taylor cone geometries, corresponding to the cases $a_1 = 1$, 0, and -1. Equation 8 has been used to generate the three prototypical cone shapes of **Figure 2**, corresponding to $a_1 = 1$, 0, and -1, respectively. The special case $a_1 = 0$ is the pure Taylor cone, characterized by a strictly conical shape, with $\Delta p = 0$.

2.3. Theoretical Studies of Neutral Drops in External Fields

When a drop of a conductor or even a dielectric is subject to a sufficiently strong external electric field, it also becomes unstable and forms pointed tips. Neutral drops form two opposite jets (**Figure 1*d***) ejecting opposite currents, so charge neutrality may be preserved through long stable emission periods (particularly in high conductivity liquids, which lose little mass). Slightly charged drops initally form only one jet (**Figure 1*d***). The literature on this subject is extensive due to its relevance in atmospheric applications (drop breakup and ion injection in the atmosphere during thunderstorms), and requires no detailed review here (Brazier-Smith et al. 1971, Ha & Yang 2000). There are currently no computations for static equilibrium shapes

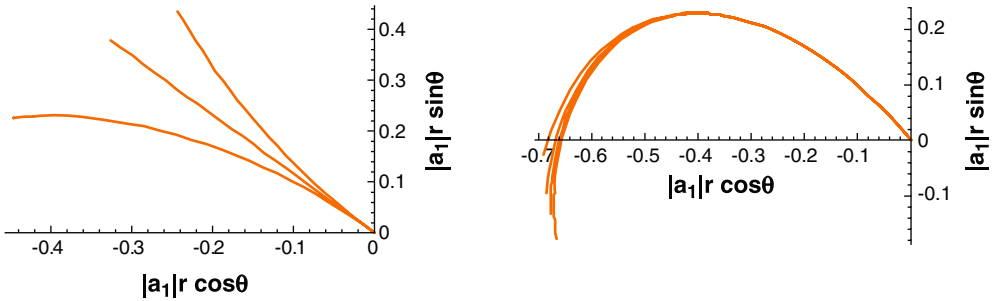

Figure 2

Shape of a static Taylor cone with lengths made dimensionless with $|a_1|^{-1}$. The left figure corresponds to $a_1 = 1$ (*top*), 0 (*middle*), and –1 (*bottom*), and keeps 15 terms in Equations 6 and 8. The right figure shows the effect of keeping fewer terms in the expansion in the case $a_1 = -1$ (15, 14, 13, and 11 terms, from *bottom* to *top*).

in conducting drops showing hysteresis phenomena, but existing theoretical studies with dielectrics are relevant because pointed tips with angles $\alpha(\varepsilon)$ that depend on the dielectric constant ε are possible equilibrium solutions (Ramos & Castellanos 1994), and the static limit of a dielectric of infinitely large dielectric constant ($\varepsilon \to \infty$) is formally equivalent to the static limit of a conductor. Stone et al. (1999) give a useful review of twentieth-century work on pointed drops. Their article makes substantial analytical progress under the assumption that the cone angle α is small, to the point of reducing the description of the shape of a dielectric drop in a uniform electric field to a first-order ordinary differential equation. This simple picture enables the determination of drop shapes in the whole range of Δp values within which pointed drops exist. Because the theory is justified only at a small tip angle, its applicability to pointed conducting drops (for which $\alpha = \alpha_T = 49.3^\circ$) is questionable and has not been pursued. Note, however, that the relation $\alpha(\varepsilon)$ predicted by its approximate differential equation is in fair agreement with exact results, even at the relatively large angles associated with the limit $\varepsilon = \infty$.

Ohmic conduction: conduction model in which the electrical conductivity is presumed to be uniform

Leaky dielectric: a medium behaving as an ohmic conductor and governed by Stokes equations ignoring fluid inertia

3. FINITE ELECTRICAL CONDUCTIVITY: OHMIC MODEL AND EXTENDED LEAKY DIELECTRIC MODEL

The perfect-conductor model used thus far permits equilibrium because all the forces acting on the interface are normal to it. The same thing happens with a perfect dielectric. Once the critical charge reaches beyond the point at which the meniscus becomes unstable, the surface moves, and its evolution can be followed in time, even with dynamic models of infinite conductivity. A tendency to form transient pointed tips in a finite time has been reported (Betelu et al. 2006), as has the formation of evolving elongated features in the tip region (Reznik et al. 2004). However, there is no evidence that infinite conductivity models can give rise to anything like the observed steady jets with characteristic dimensions much smaller than the meniscus. The development of very fine and steady jets at the apex of Taylor cones is in fact known from experiments to depend strongly on electrical conductivity, with a tendency for the jet diameter to shrink toward zero approximately as a negative power of the electrical conductivity. It is therefore clear that a model for charge transfer is necessary to obtain steady cone-jet structures. The situation then becomes much richer as tangential fields may be present, leading to shear forces on the charged surface and tangential motion that is eventually responsible for jet formation. To date, all the theoretical literature on dynamic Taylor cones has assumed that the liquid has a uniform electrical conductivity (ohmic conduction) unaffected by the flux of charge $\mathbf{j}''$ ($\mathrm{Cm^{-2}s^{-1}}$). $\mathbf{j}''$ is taken to be proportional to the local electric field $\mathbf{j}'' = \mathrm{K}\,\mathbf{E}$, through a single scalar constant K, the electrical conductivity. The combination of this model for charge transport with Stokes's equations for the fluid motion is often called the leaky dielectric model, originally introduced by Taylor (1966) and previously covered in two Annual Reviews articles (Melcher & Taylor 1969, Saville 1997). Saville explores the limitations of the ohmic model and proposes a more general model that includes what he denotes as electrokinetic effects. These replace the hypothesis of constant electrical conductivity by the assumption that ions have constant mobility

Ambipolar diffusion: charge transfer mechanism in electrolytes where space charge is very small

and exist at concentrations governed by transport equations, including the ionization-recombination reaction $AB = A^+ + B^-$. He concludes that "none of the experimental studies show major electrokinetic effects despite the indications of the scale analysis." The pure ohmic model also appears to hold with Taylor cone-jets, but, as argued below, an exception arises at low flow rates in liquids having high dielectric constant and low viscosity, such as water and formamide (Fernández de la Mora & Loscertales 1994). In these cases, drastic departures from the constant conductivity limit occur, involving substantial reduction of salt concentration in the cone-jet transition region (Section 4.7).

Charge transport near the tip of a Taylor cone is peculiar because liquid convection upsets the charge distribution dictated by purely electrostatic considerations, so internal currents and fields develop in an attempt to restore them. Because the surface charge increases as the cone tip is approached, this generally means that the internal fields feed net charge to the tip region by conduction. This requires a flow of positive charge from the bulk into the boundary and of negative charge from the boundary to the interior of the liquid. But there is no reservoir of negative charge on the boundary, so this process requires the depletion of negative charge from a layer adjacent to it. Simple considerations based on the net charge that eventually reaches the interface determine the depth of this depleted layer, showing that it may be larger than the Debye length under certain circumstances. Two possible scenarios would then permit net charge transport from the bulk to the boundary through this depleted region. The depleted layer may be almost neutral, in which case transport would occur via ambipolar diffusion through a progressively thickening layer depleted of both ion types. Alternatively, one would encounter a space charge–dominated region possibly thicker than the Debye length.

3.1. Rarefaction Fronts

Fernández de la Mora & Larriba (2007, in preparation) explored what happens when the convective evolution of the liquid parallel to the charged interface is replaced by a simple time variation. In the limit of a fully ionized liquid with only one ion of each polarity (at concentrations n^+ and n^-), the governing equations are

$$n_t^+ + [n^+\omega^+E - n_x^+kT\omega^+/e]_x = 0, \tag{10}$$

$$n_t^- + [-n^-\omega^-E - n_x^-kT\omega^-/e]_x = 0, \tag{11}$$

and

$$E_x = e(n^+ - n^-)/(\varepsilon\varepsilon_o), \tag{12}$$

where E is the field normal to the surface, subscripts t and x denote partial derivatives with respect to the spatial and time variables, ω denotes the ion mobility, and the superscripts + and – refer to species of positive or negative polarity. These equations can be written in dimensionless form after introducing the Debye length λ (Equation 14), the uniform ion concentration N prevailing far from the interface, and the dimensionless variables:

$$y = x/\lambda; \quad \lambda^2 = \varepsilon\varepsilon_o kT/(Ne^2); \quad F = e\lambda E/(kT); \quad 2\nu = (n^+ + n^-)/N \quad (13\text{–}16)$$

$$\tau = t\,\omega^+ kT/(e\lambda^2); \quad \varphi = \omega^-/\omega^+. \quad (17,18)$$

Using ν and F as the only dependent variables, the order of the system increases, but the higher-order derivatives F_{yyy} that arise can be removed by subtracting Equations 10 and 11 and integrating once in y, which results in an integration constant C(t). The result is a pair of second-order equations similar to those resulting from the usual assumption of quasi-neutrality, yet retaining space charge effects in full:

Charge relaxation: convection-driven departures of the surface charge density of a medium of finite conductivity away from the value it would have on a perfect conductor

$$\nu_\tau(1 + \varphi^{-1}) + \tfrac{1}{2}F_{y\tau}(1 - \varphi^{-1}) + [FF_y - 2\nu_y]_y = 0 \quad (19)$$

$$F_\tau + (F\nu - \tfrac{1}{2}F_{yy})(1 + \varphi) + (\tfrac{1}{2}FF_y - \nu_y)(1 - \varphi) = C(\tau). \quad (20)$$

The boundary conditions deep into the fluid bulk ($y \to -\infty$) are $n^+ = n^- = N$; hence, $\nu = 1$, $F_y = 0$. At the free boundary $y = 0$, the field is assumed to be fixed externally, $F(0, \tau) = F_o(\tau)$, and there is no flux of either positive or negative ions: $n^+F - n_y^+ = 0$; $-n^-F - n_y^- = 0$, as the ions cannot jump into the gas. It follows that $C(\tau) = F_\tau(0,\tau)$, which fully determines C(t) from the boundary condition fixing $F(0,\tau) = F_o(\tau)$. In summary, the evolution is governed by Equations 19 and 20, with $C(\tau)$ given in Equation 21 and boundary conditions in Equations 22–25:

$$C(\tau) = dF_o(\tau)/d\tau = F_o'(\tau) \quad (21)$$

$$FF_y - 2\nu_y = 0,\ F = F_o(t) \ \text{ at } \ y = 0; \quad \nu = 1, F_y = 0 \ \text{ as } \ y \to -\infty. \quad (22\text{–}25)$$

The most natural initial condition for an initially uncharged surface is that the ion concentration is uniform, and the field is spatially uniform and identical to the value impulsively established at the boundary (Equations 26–28):

$$\nu(y) = 1,\ F(y) = F_o(0) \ \text{ at } \ \tau = 0; \quad F_\tau + (1+\varphi)F = F_o'(\tau), \ \text{ as } \ y \to -\infty. \quad (26\text{–}28)$$

The field at infinity is related to that at the interface by the simple linear charge relaxation Equation 28, with the same relaxation time $t_{rel} = \varepsilon\varepsilon_o/[Ne(\omega^+\omega^-)]$ governing the purely Ohmic limit. Equation 28 also shows that time-varying external fields produce nonzero internal fields. This is the situation of a Taylor cone, where the external field increases as the cone tip is approached.

3.1.1. Linearly increasing external electric field. We consider the problem $F_o(\tau) = 0$ for $\tau < 0$; $F_o(\tau) = \alpha\tau$ for $\tau > 0$, where, within a few relaxation times, the electric field deep inside the liquid approaches the uniform value $F \to F_\infty = \alpha/(1 + \varphi)$ as $y \to -\infty$. The numerical solution to Equations 11–17 was determined by Larriba for $\varphi = 1$, as shown in **Figure 3** for $\alpha = 0.35$ as a series of profiles $2/(1 + F(y)/F_\infty)$, $n^+(y)/N$, and $n^-(y)/N$ at varying times. One sees a progressive depletion of both positive and negative ions from the boundary, with a wave propagating toward the bulk. After a sufficiently long time, the wave develops a self-similar shape in terms of the variable $\eta = y + F_\infty\tau$.

The most interesting aspect of the solution is the fact that the positive ions are removed completely from the left end of the wave, so that negative ion transport to

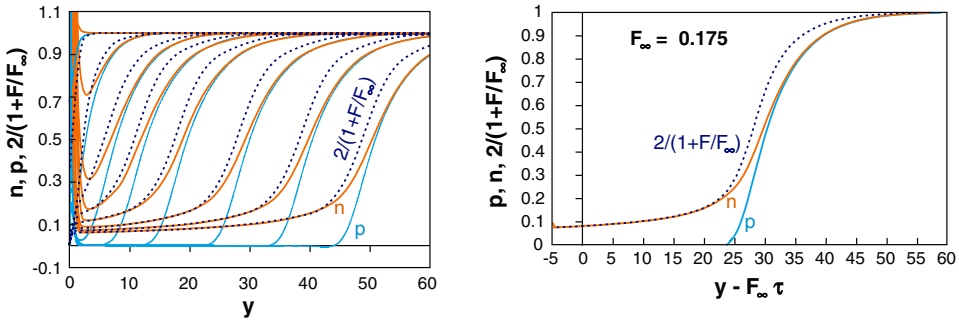

Figure 3

Time evolution of the profiles for $p = n^+/N$, $n = n^-/N$, and $2/(1 + F/F_\infty)$. The left figure uses the dimensionless distance y (13) as the horizontal variable, and corresponds from right to left to $\tau = 300, 240, 180, 120, 80, 50, 20, 2$. The right figure represents the same data for the four longest times as a function of the similarity variable $\eta = y - F_\infty\tau$. $F_\infty = \alpha/2'$ $\varphi = 1$.

the wall takes place dominantly by space charge. In the space charge region diffusion is negligible so that νF (hence FF') is constant, whereby with a suitable origin of η, $F(\eta) = -F_\infty + (-4F_\infty\eta)^{1/2} + \cdots$ and $\nu(\eta) = (-F_\infty/\eta)^{1/2} + \cdots$ Although this space charge region may extend over many Debye lengths, the absence of positive ions in the depleted region has no effect on the net flux of charge, which is determined at infinity, where bulk concentrations prevail. The rarefaction front can therefore be found by first solving the constant conductivity problem to obtain the internal field near the interface. This determines the propagation velocity and hence the location of the front at all times. The approach holds equally for a different time dependence of the field $F_o(\tau)$ at the surface. Without rigorous analysis, Fernández de la Mora & Loscertales (1994) have applied the same idea to a model Taylor cone.

4. STEADY TAYLOR CONE-JETS AT HIGH ELECTRICAL CONDUCTIVITY

4.1. Onset Voltage and Electrical Discharges

The early studies of Zeleny (1915, 1935) clarified that the critical voltage for ES formation scales as $\gamma^{1/2}$, as required by the balance $\varepsilon_o E^2/2 \sim \gamma/r$ between electrostatic and capillary pressures. He also studied the essentially equivalent effect of the pressure jump across the meniscus on the required critical voltage. Zeleny (1915) was interested in electrical discharges, and noted what has subsequently escaped many others: that high surface tension liquids such as water have ES onset voltages large enough to strike electrical discharges prior to cone-jet formation. His work suggests the remedy of using CO_2 instead of air. Other high-voltage breakdown gases (electron scavengers) such as O_2 and SF_6 (Smith 1986) serve a similar purpose, which explains why air is a much better electrospraying medium than nitrogen, and why noble gases (particularly He) (Michelson 1990) are such poor choices. The same reasons generally

make negative ESs harder to stabilize than positive ones. Similar considerations explain why ESs are more easily stabilized in gases at both high and low pressures. Taylor (1964) made Zeleny's picture more quantitative by assuming that the meniscus shape is conical and determining the cone angle. Taylor's model confirms Zeleny's scaling for the critical voltage in terms of a characteristic dimension of the electrode supporting the meniscus (say the diameter d of a capillary tube),

$$V \sim (\gamma d/\varepsilon_o)^{1/2} \tag{29}$$

with weak corrections, varying as ln(h/d) with the distance h between the needle tip and a ground electrode. The same scaling results for a drop at the Rayleigh limit. More importantly, Taylor's potential (Equation 2) also describes completely the electric field in the vicinity of the apex, without any unknown parameter.

4.2. Cone Angle vs Taylor Angle, Space Charge, and Spray Structure

A matter of concern to the theorist attempting to extend Taylor's description to the jet region is the fact that although real Taylor cones may be tweaked into adopting Taylor's angle, far more often they show substantially smaller values. One reason for this is that Taylor's model assumes that the axis $\theta = 0$ contains no charge, but in fact it carries a charged jet whose repulsion pushes back the cone into a smaller angle. Space charge associated with the spray of drops formed after jet breakup has an even larger effect due to the lower velocity of the drops. For high conductivity liquids, when the jet is very narrow, its length prior to breakup is small compared with that of the liquid cone, and the drops have insignificant inertia. Hence, the spray originates essentially at the cone apex. In this case, if all the drops have the same electrical mobility (say, by being involatile and having identical initial charge q and diameter), then it is possible to have an analytical description of the liquid cone and the spray involving a liquid cone in the region $\pi < \theta < \pi - \alpha$ with an equipotential surface at $\theta = \pi - \alpha$, and a spherically symmetric spray in the region $\beta < \theta < 0$. The corresponding electrical potential ϕ_s and drop number density n within the spray are:

$$\phi_s(r) = a(2\gamma r/\varepsilon_o)^{1/2}, \tag{30}$$

$$n(r) = 3a\, q^{-1}(\gamma\varepsilon_o/8)^{1/2}\, r^{-3/2}. \tag{31}$$

Because ϕ_s depends on the polar radius r exactly as Taylor's potential (although with no angular dependence), it is possible to match the field within the spray with a slightly modified form of Taylor's field in the charge-free space: $\phi \sim r^{1/2}\ \{mP_{1/2}(\cos\theta) + n\, P_{1/2}[\cos(\pi - \theta)]\}$, where the new term $P_{1/2}[\cos(\pi - \theta)]$ enables the charge to be present at $\theta = 0$. The matching of potentials at $\theta = \beta$ uniquely determines the constant a in Equations 30–31, and the spray angle β as functions $a = a(\alpha)$ and $\beta = \beta(\alpha)$ of the liquid cone angle α. α is now a free parameter of the problem, which can take any value smaller than α_T, and tends to α_T in the space charge-free limit when $\beta = a = 0$. The quantity a^2 is also interpreted as the dimensionless spray current per unit solid angle. In spite of its simplicity, this model agrees surprisingly well with experiments, which show not only the double-cone structure assumed,

but also quantitative agreement between the observed and predicted $\alpha(\beta)$ relation (Fernández de la Mora 1992). In addition to its rationalization of the small cone angles, this model permits estimates of the position dependence of the spray density n, which is of considerable interest when sampling an ES through the entry orifice of a mass spectrometer. In this case, the solvent is highly volatile and the drops evaporate quickly, giving rise to ions. The relevant electrical mobility would then be that of these ions rather than the initial drops. The model also demonstrates the resistance to charge transport in the gas region, and suggests there is a limit to the maximum possible transmitted current. Sprays where drop inertia is substantial are far from conical and have been described by Tang & Gomez (1994 a, 1996) and Gañán-Calvo et al. (1994). A fascinating feature when various sizes or charge states are present (almost always) (de Juan & Fernández de la Mora 1997) is their spatial separation. The phenomenon may be explained by the instability of the line of initial collinear drops produced by the jet breakup. Any slight displacement from the axis leads to rapid ejection at a rate that depends only on mass/charge, as viscous drag is initially irrelevant. In sprays with main and satellite drops, one can clearly distinguish the satellites in the periphery of the spray, with a drop-free annulus between the satellites and the main drops. The imposing theoretical richness of the problem of charged jet breakup (ignoring the subsequent drop spread) can be fathomed through the bibliography of López-Herrera et al. (2005).

4.3. Drop Monodispersity

Another widely quoted feature of ESs was the narrow size distribution of the drops produced by the regular breakup of the jet. This claim rested on the striking spray colors often seen (**Figure 1*a***), but it was not seriously quantified until the systematic studies of Cloupeau & Prunet-Foch (1989, 1990, 1994) and Tang & Gomez (1994a,b; 1995; 1996).

4.4. Stability Island

As late as 1986, the knowledge about ESs was rather qualitative. The common mention of an impossibility to ES high conductivity solutions had been long refuted by Zeleny's work with acidified water, where the control was through the height of the meniscus with respect to the reservoir of liquid (the pressure jump Δp). Smith (1986) clarified that the same notion applied to situations in which the spray was controlled through the flow rate of liquid Q fed to the Taylor cone. Smith noted the need to use decreasing liquid flow rates at increasing electrical conductivities, including almost infinitesimal values in concentrated electrolytes. Cloupeau & Prunet-Foch (1989) described in greater detail the existence of a finite island of stability in terms of the two key controlling parameters Q and the voltage V applied to the needle with respect to a neighboring electrode. The minimum voltage or onset voltage already discussed is in fact Q dependent. Little is known about why there is a minimum or a maximum flow rate beyond which the cone-jet is no longer stable. The minimum flow rate is considered in Section 4.7. It is of great practical interest because it produces the smallest possible jets, and their breakup into drops is most regular near Q_{min}

(Rosell & Fernández de la Mora 1994). The probable reason noted already for Q_{max} (Section 4.2), is that the gas eventually becomes unable to pass the increasing flux of spray drops injected by the liquid tip. The maximum voltage is associated with the appearance of either multiple cone-jets or electrical discharges. The range of voltages V_{max}/V_{min} is a quantity of order one.

4.5. Length Disparity and Decoupling of the Jet from the Electrostatic Variables

The types of variables affecting the ES problem include voltage and electrode geometry (electrostatic parameters), liquid flow rate Q, and physical properties of the liquid (density ρ, surface tension γ, viscosity μ, and dielectric constant ε, among others). Mapping this vast parameter range experimentally is almost unthinkable. However, Fernández de la Mora & Loscertales (1994) discovered that the task was manageable for liquids of high conductivity, for which the jet diameter d_j is many times smaller than the diameter d of the capillary tube supporting it (**Figure 1*a***), whereby d becomes approximately irrelevant for all purposes other than fixing the onset voltage. All other features affecting the electrostatic problem are equally irrelevant—not only the shapes and positions of the emitting capillary and other electrodes, but, to a first approximation, also the needle voltage V. In other words, the jet structure and charge depend almost exclusively on the local characteristics of the cone tip, as would be expected from anything issuing locally from a singularity. This simplification is very useful, but, as shown by the careful measurements of Smith et al. (2006), it is not exact.

4.6. Scaling Laws for the Jet

For a given liquid, experiments by Fernández de la Mora & Loscertales (1994) showed that the jet current and shape depend almost exclusively on the flow rate Q, with a dependence close to $I \sim Q^{1/2}$. Varying the electrical conductivity K further showed that $I \sim (KQ)^{1/2}$. This surprisingly simple result is readily rationalized. Charge conservation at the interface requires that the surface current $I_s = 2\pi\sigma R u_s$ (σ is the surface charge density, R the local meniscus radius, and u_s the surface velocity) convected toward the apex increases by incorporating the net flux of charge $K\mathbf{n}.\mathbf{E}_i$ reaching the surface (with normal **n**) from the fluid interior as a result of the internal electric field $\mathbf{E}_i$. Hence, $dI_s/ds = 2\pi R\, K\mathbf{n}.\mathbf{E}_i$, where s is the coordinate along the surface. Writing $\sigma = \varepsilon_o(\mathbf{E}_o - \varepsilon\mathbf{E}_i).\mathbf{n}$, and using $dt = ds/u_s$ for the convective time, this gives a simple linear charge relaxation equation, where σ tends toward the electrostatic limit $\varepsilon_o\mathbf{E}_o.\mathbf{n}$ when the flow time is large compared with the charge relaxation time $\varepsilon\varepsilon_o/K$. However, σ may fall substantially below this electrostatic limit. We denote such departures as charge relaxation effects, which may be measured by the ratio between $\varepsilon\mathbf{E}_i.\mathbf{n}$ and $\mathbf{E}_o.\mathbf{n}$. Gañán-Calvo et al. (1997) used the term charge relaxation in the different sense of lack of space charge effects, and concluded that no charge relaxation can possibly occur because net charge quickly relaxes to the surface. The space charge issue has already been considered more generally in Section 3. For present purposes it suffices

to note that the ohmic conduction model used by most authors, including Gañán-Calvo and colleagues, does not allow for space charge effects. The claim of lack of space charge effects is therefore tautologic within that model. However, the related claim of lack of charge relaxation (as we define it) is unjustified, as first shown by the analysis of Fernández de la Mora & Loscertales (1994), and even more convincingly demonstrated by the subsequent detailed numerical calculations of Higuera (2003).

In conclusion, the surface is essentially equipotential down to the point where the meniscus cross section is small enough (large velocities) for the convective time to be of the order of $\varepsilon\varepsilon_o/K$. Subsequently, the finite electrical conductivity is unable to replace the surface charge removed by convection to keep it close to the electrostatic value, and the surface current freezes. Downstream from that point, Taylor's equilibrium can no longer be satisfied and the cone turns into something different, evidently a jet. Taking the surface to be conical with angle α_T, and the flow to be a spherically symmetric sink with a polar distance R to the apex, freezing occurs when the flow time $R^3/Q \sim \varepsilon\varepsilon_o/K$, at which point the surface convection current is of the order $I_s \sim (\gamma KQ/\varepsilon)^{1/2}$. This dependence on KQ is as found experimentally. This model suggests the following scaling laws for the jet current and diameter

$$I = g(\varepsilon)(\gamma KQ)^{1/2} \tag{32}$$

$$d_j = G(\varepsilon)r^*; \quad r^* = (Q\varepsilon_o/K)^{1/3}, \tag{33,34}$$

where the functions g and G depend only on the dielectric constant of the liquid. [Note that the definitions of r^* and the coefficients $G(\varepsilon)$ and $g(\varepsilon)$ used here differ by factors $\varepsilon^{1/3}$ from those of Fernández de la Mora & Loscertales (1994).] The identification of the total current with the freezing value of the surface current results from the fact that the sum of the surface convection current and the bulk conduction current is constant, the latter dominating upstream in the cone, the former being the only charge transport mechanism available in the downstream regions of the jet. The conspicuous absence of the density ρ and the viscosity μ from these laws is at first surprising, but the approximate validity of Equation 32 has been confirmed by several independent experimental studies for numerous liquids covering the range $2 < \varepsilon < 182$ (Chen & Pui 1997, Fernández de la Mora & Loscertales 1994). Gañán-Calvo et al. (1997) also confirmed these results for liquids of either high electrical conductivity or high viscosity, but report otherwise a different behavior. Their analysis absorbing the dependence on ε into new variables leads to a concrete form for the dimensionless current function $g(\varepsilon)$. Its fair agreement with experimental values is surprising because ε survives in Laplace's equations for the electrical potentials.

The agreement between authors is not as good regarding the experimental values of the function $G(\varepsilon)$ for the jet diameter, particularly for large ε. Testing Equation 33 (Chen & Pui 1997, Gañán-Calvo et al. 1997, Rosell & Fernández de la Mora 1994) involves greater complexity, as the jet is not cylindrical but shrinks continuously downstream. Furthermore, what is generally measured is not the full jet shape, but the diameters of the drops into which it finally breaks, which at best are related to the jet diameter at the breakup point. This experimental circumstance has led to

a range of scaling laws for the jet diameter, with the general form $d_j \sim r^* \eta^n$. But because n is a small number and the dimensionless group $\eta = (\rho K Q/\gamma \varepsilon \varepsilon_o)^{1/2}$ is of order one, the differences are slight and difficult to resolve by experiment. According to a remarkable study by Gamero-Castaño & Hruby (2002), Gañán-Calvo's length $r_G \sim \eta^{1/3} r^*$ is a better predictor of d_j than r^*. These authors manage to measure in a vacuum what seemed immeasurable: the jet voltage, speed, and diameter at the breakup point. However, the theoretical reasons given by Gañán-Calvo for the choice of r_G are less persuasive than those later contributed by L. Cherney (private communication) in favor of the slightly different choice, $d_j \sim r_C = r^* \eta^{2/5}$, based on the predicted asymptotic jet shape (Equation 35) and its length at breakup, which is derived from the known growth rate of the capillary instability in uncharged jets. The asymptotic jet shape is determined by an argument first proposed by Gañán-Calvo, where an energy equation is derived from a momentum balance downstream from the region where the jet current is purely convective (hence, dissipation due to electrical conduction disappears). Gañán-Calvo also argued that the axial electric field is that of Taylor, essentially unmodified by the presence of the jet. Further support for these important points has been provided by others (Cherney 1999, Gamero-Castaño & Hruby 2002, Higuera 2003), so the jet asymptote (Equation 35) appears to be as firmly established as the Taylor cone, although the current carried and the breakup diameter are determined in the transition region and must be found numerically.

Electrospin: to draw a continuous fiber instead of a spray from a nonbreaking jet issuing from a Taylor cone

$$p + 1/2\, \rho u^2 + I\phi/Q = \text{Constant} \tag{35}$$

In Equation 35, p is the pressure inside the jet, u is its velocity (taken to be radially uniform at an axial position x), and ϕ is Taylor's potential (Equation 2) specified at $\theta = 0$ (where $r = x$): $\phi \sim -(\gamma x/\varepsilon_o)^{1/2}$. Sufficiently downstream, $p \ll 1/2\, \rho u^2$, and Equation 35 fixes a very slowly varying jet radius, $R \sim x^{-1/8}$. On the assumption that this jet is unstable with the same growth time as uncharged cylindrical jets, x at breakup scales as $u(\rho R^3/\gamma)^{1/2} \sim (Q^2 \rho/R\gamma)^{1/2}$, which, once inserted into the $R \sim x^{-1/8}$ law, leads to Cherney's scaling.

In conclusion, with some small corrections noted by Higuera (2003), viscosity and inertia are relatively irrelevant in the apex region, where the jet is formed and its current is fixed, and where the characteristic diameter and current are given by Equations 33 and 32. However, the breakup process determining the final jet diameter involves inertia, hence the appearance of ρ in Cherney's length. The jet breakup into drops also involves viscosity in a well-known fashion, such that the ratio of drop to jet size increases in more viscous liquids (Rosell & Fernández de la Mora 1994).

While it was originally believed that the breakup occurs at a voltage much closer to the needle voltage than to ground, Gamero-Castaño & Hruby (2002) have shown that the jet voltage may drop almost to ground, even in moderately viscous liquids such as tributyl phosphate. The same must happen in more viscous materials, including the rather long electrified glycerine jets described by Zeleny (1917) and Taylor (1964), and their recent analogs which never break and are widely used to electrospin continuous fibers (Hohman et al. 2001a,b).

4.7. Theoretical and Numerical Analysis of the Transition Region

Pure theory has been useful principally to resolve the cone and jet asymptotes, as noted above. Several strictly theoretical articles by Gañán-Calvo (1997, 1999, 2004) have subsequently addressed the asymptotic universal scaling laws in electrospraying, the general scaling theory for electrospraying, and the universal scaling laws for surface charge in electrostatic spraying. These studies have generally relied on the dubious assumption of lack of charge relaxation effects. Furthermore, the diversity of hypotheses brought and conclusions drawn in these papers, and the unclear consistency among them and with the real problem are not entirely transparent.

Several computational efforts aimed at determining the full cone-jet structure have been more elucidating. Some have successfully attacked the full problem from the needle to the final jet region (before breakup), even though the numerical stiffness resulting from the presence of two highly disparate length scales limits the possibility of progress to relatively low electrical conductivities. Most useful among these studies is the Ph.D. thesis of Carretero-Benignos (2005), which includes detailed cone-jet structures as well as comparisons with experimentally measured global quantities. Its publication in article form would be most desirable. Higuera (2003) followed the alternative path of restricting the numerical analysis to just the apex region, using the cone and jet asymptotes as boundary conditions. This approach is consistent with the singular nature of the high conductivity limit, and naturally separates its inner and outer regions, moderating the stiffness difficulty and enabling the study of arbitrarily high conductivities. Higuera finds that liquid viscosity is not as irrelevant as implied by prior experiments. He recovers the $I \sim Q^{1/2}$ law, but only as an approximation. Although quantitative agreement with experiments remains to be addressed, his successes to date open up new dimensions in these investigations, as he can compute characteristics of jets only 10 nm in diameter that are immeasurable. For instance, the maximum normal electric field E_{max} on the gas side of the meniscus is vitally important for studies on ion evaporation from Taylor cones. If the only relevant characteristic length were r^* (Equation 34), E_{max} would be given by Equation 36 (Gamero-Castaño & Fernández de la Mora 2000). The approximate validity of this scaling was confirmed by Higuera's computations, which yield $\varphi(64.92) = 0.76$ in the case of propylene carbonate (I. Guerrero, R. Bocanegra, J. Fernández de la Mora, F.J. Higuera. 2006. Ion evaporation from Taylor cones of propylene carbonate mixed with ionic liquids. *J. Fluid Mech.* Submitted).

$$E_{max} = \varphi(\varepsilon)(\gamma/r^*\varepsilon_o)^{1/2} \tag{36}$$

Due to convergence difficulties, Higuera's calculations have not yet shed light on the island of stability. Furthermore, certain paradoxes remain. For instance, in the comparisons with experiments attempted by Guerrero et al. (2006), the calculations converge at dimensionless liquid flow rates much smaller than those for which stable real cones can be found in reality. It is not yet clear if the low flow rate solution found is unstable, or whether this anomaly reflects a deficiency of the constant conductivity model used. In addition, numerical convergence is not achieved at the larger flow rates at which real cone-jets are observed. As a result, there is often only a narrow

region or no region at all of parametric space where calculations and observations coexist.

4.8. The Minimum Flow Rate

We have noted that the minimum flow rate Q_{min} at which a cone-jet can be stabilized is of considerable practical importance as it determines the diameter of the thinnest jet (or the highest surface electric field) that can be achieved with a given solvent. Existing theory based on ohmic conduction has been of little help in predicting Q_{min}, so theoretical insights will first be sought from more general considerations. We shall confine this discussion to the case when the meniscus is positively charged and no ions evaporate directly from the liquid surface so that the total spray current is first carried downstream by the jet and then by the drops. The surrounding medium will be taken to be an insulator, so no current of negative charges will flow upstream. If the capillary conveying the liquid to the meniscus is metallic, the field inside it vanishes, and the positive and negative ions contained in solution move at identical speeds and only by convection, bringing in equal flows of negative and positive charge (I^- and I^+). In the simplest case of an electrolyte containing only one kind of singly charged positive and one negative ion at initial concentration n, $I^+ = -I^- = neQ$, where e is the elementary charge and Q the liquid flow rate. An uncharged jet would transmit the full positive and negative charges with no net current. A positively charged jet will transmit the full I^+, but only part of the negative charge flux, the rest being neutralized at the electrode. At best, when the whole negative flux is neutralized, the total current will be $I = I^+$, providing the upper limit for the current:

$$I < I_{max} = neQ \tag{37}$$

The limit $I = I_{max}$ will be referred to as the complete charge separation limit. This result assumes that the electrode does not release metal ions into the solution, a point easily realizable in practice by using noble metals. Fernández de la Mora and Loscertales (1994) tested Equation 37 against their experimental data and saw that it holds in all cases. Furthermore, for polar liquids such as water and formamide, the inequality approaches an equality near Q_{min}. For other less polar or more viscous substances the minimum flow rate arises at conditions quite removed from the limit of Equation 37, the more so the higher the ion concentration. Chen & Pui (1997) re-examined the issue for acidified aqueous solutions without confirming the earlier claim. However, Tang & Gomez (1995) found that the minimum flow rate and current for ESs of deionized water in CO_2 gas fall quite close to complete charge separation conditions for one of the two distinct steady cone-jet regimes they observed, which they identified with the conventional cone-jet. Remarkably, their other regime achieves flow rates far smaller and currents far larger than permitted by Equation 37, leading to the generation of substantially smaller drops than can be produced in ordinary cone-jet mode. This anomaly was convincingly explained as owing to the presence of a mild electrical discharge, not only providing strong evidence in favor of Equation 37, and showing how to reverse it (via a negative current flowing upstream),

but also beautifully illustrating the rich possibilities of interplay between ESs and electrical discharges.

The limit of complete charge separation is evidently rather extreme. For a NaCl solution, the drops would contain only Na^+ with no Cl^- counterions at all. The same would happen in the final regions of the jet, where the bulk fluid would contain no ions of either sign, the positive charge would reside entirely on the surface, and the liquid would have zero electrical conductivity. In other words, the whole flow field would have been invaded by the rarefaction front described in Section 3.1. In conclusion, the work of Tang & Gomez confirms the anticipated need to go beyond the Ohmic model to predict Q_{min} in water-like liquids. However, these measurements do not provide direct support for the ideas discussed in Section 3.1, because the Debye length ($\sim$6 μm, inferred from the reported $n \sim 4.81\ 10^{21}\ m^{-3}$) is comparable to the drop diameter ($\sim$5μm measured at the point of complete charge separation).

A one-dimensional model for the fate of the ions in a flow section A with convective velocity U and electric field E would give $I^{\pm} = neA(\omega^{\pm} E \pm U)$. Once past the entry tube and in the presence of an electric field, the positive ions would be accelerated and the negative ions decelerated by the field, with n remaining the same for both (no space charge). The flow rate can be reduced up to the point where $\omega^- E = U$. At lower flow rates the negative ions would drift upstream to be removed entirely from the downstream regions of the flow field, a situation that cannot be sustained due to space charge. The limit $\omega^- E = U$ corresponds to complete charge separation, as the negative ions remain fixed in space and their downstream flux is zero. The same happens in a spherically symmetric situation such as one would encounter in a cone. On the other hand, when negative ions are fed at the tip of the cone with a mild discharge, as in the experiments of Tang & Gomez (1995), a change of sign of I^- can take place, allowing for lower flow rate situations ($U < \omega^- E$) than before, as observed by these authors.

Another special case of complete charge separation is encountered in the purely ionic regime of liquid metals, where the electron cloud remains fixed in the Taylor cone as the metal ions drift through it toward the tip. In the purely ionic regime of molten salts A^+B^- (Section 6) the emissions ions include the bare cation A^+ as well as the dimer ion $A^+(AB)$. The situation is nonetheless analogous to the complete charge separation case because the proportion of both constituents [A^+ and $A^+(AB)$] is approximately independent of flow rate, and the ratio of current over flow rate is constant and equal to the volumetric charge density (as in Equation 37).

For the many substances such as ethylene glycol for which complete charge separation is not approached at Q_{min}, another explanation is needed for Q_{min}. The experiments of Fernández de la Mora & Loscertales (1994) and Chen & Pui (1997) show that, for a given liquid, KQ_{min} is approximately constant independently of the electrical conductivity. The minimum emitted current I_{min} is then almost independent of K, and the stability island can be represented for a given fluid in terms of the single parameter KQ. This quantifies the previous qualitative result of Smith (1986) that more conducting liquids call for decreasing flow rates. A more general, strictly experimental, finding is that the dimensionless group $\eta_{min} = (\rho K Q_{min}/\gamma\varepsilon\varepsilon_o)^{1/2}$ is of the order of 1 (Chen & Pui 1997, Fernández de la Mora & Loscertales 1994). There

is no general rigorous theoretical justification for this result. However, a tentative explanation is suggested by Higuera's observation (private communication, 2006) that, in Cherney's scenario (as presented in Section 4.6), the jet length becomes comparable to its diameter. Accordingly, there should not be a jet at $\eta \sim 1$, although a jet is essential to the whole reasoning, and is also seen in reality. For large ε, a possible answer to this objection can be based on the fact that Cherney's scales for the diameter d_j and the length L_j of the jet at its break-up point are really

$$d_j/r^* \sim \varepsilon^{1/5}\eta^{2/5}; \quad L_j/r^* \sim \varepsilon^{2/5}\eta^{4/5}. \tag{37,38}$$

Note that this result for d_j and L_j is independent of ε because the two groups involved, r^* and $\delta = \varepsilon^{1/2}\eta = (\rho KQ/\gamma\varepsilon o)^{1/2}$, are both independent of ε. This is clear because ε appears neither in the energy conservation Equation 35 [except in I, but $g(\varepsilon)$ is known experimentally to be insensitive to ε], nor on Cherney's capillary wave growth rate argument determining the jet length. Therefore, at large ε, a moderately slender ($L_j/d_j \sim \varepsilon^{1/5}\eta^{2/5}$) jet exists even at $\eta = 0(1)$, although its brevity suggests two possible mechanisms for cone-jet destabilization at decreasing η. Either the jet disappears, making a cone-jet impossible, or the merging of the axial scales L_j for breakup and L_I for the surface current to reach its asymptotic value (generally believed to be large compared to r^*) destabilizes the jet.

Provided the ES current depends only on the product KQ (as observed), and that $n \sim K$ (as is the case of polar liquids at low ion concentration), a theroretical justification of the scaling $KQ_{min} = \text{constant}$ (or $\eta_{min} = \text{constant}$) also arises naturally in the limit of complete charge separation.

5. POINTED CHARGED DROPS AND THEIR PROGENY

No published analytical or computational hydrostatic information is currently available on either the hysteresis ratio q_o/q_R, the drop shape, or the associated dimensionless pressure jump $R\Delta p/\gamma$ for charged pointed drops in a field-free region. However, there have been many measurements on the relation q(R) at which instability arises, and on the loss of charge and mass following it, as well as scanty information on the size and number of the daughter drops produced (see Fernández de la Mora 1996 and Li et al. 2005 for a review of these studies).

Several remarkable published images of charged drops supporting one or two Taylor cones have also generated a lot of interest. The one reproduced in **Figure 4*a*** (Gomez & Tang 1994) represents a heptane drop caught in the middle of a Coulombic fission, shortly after having been produced by ES atomization from a much larger meniscus. This early image was widely circulated and reproduced and played a large role in persuading the ES community of the universality of the Taylor cone formation mechanism, irrespective of the supporting geometry. It also illustrated the effectiveness of the Coulombic explosions of ES drops to produce smaller and smaller daughter drops, as the image resolves daughter drops with radii approximately 10 times smaller than the mother drop. Many practitioners of ESMS have tended to assume that subsequent Coulombic fissions of the various generations of daughter drops would continue to undergo a 10-fold size reduction in each new generation. The issue is central to

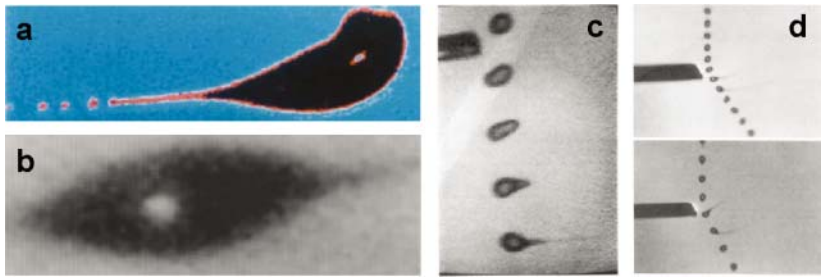

Figure 4

Early images of charged drops undergoing Coulomb explosions. Parts (*a*) and (*b*) are for heptane drops [about 60 μ and 30 μm in diameter, respectively; from figures 6a and 8 of Gomez & Tang (1994)]. (*c*) **Figure 5** of Hager et al. (1994). (*d*) **Figure 2** of Hager & Dovichi (1994) shows acetone drops charged by passing through an electrical discharge region. Only part (*b*), which corresponds to a negligible external field, shows a symmetric explosion.

ESMS, but it remains unresolved. The lack of symmetry of the Gomez-Tang drop, its relative proximity to the electrospraying needle, and the presence of neighboring charged drops from the ES indicate that the drop is not in a field-free environment. **Figure 4*b*** is from the same Gomez-Tang article. It has received far less attention, but it was the first published image of an explosion with two symmetrically opposed Taylor cones. Note that the aspect ratio (polar over equatorial lengths) is about 3, much less than the value ∼4 recently seen by Achtzehn et al. (2005) (**Figure 1*b***). A subsequent study by Hager & Dovichi (1994) developed an ingenious technique of periodic drop generation and passed them through the vicinity of a sharp tip undergoing an electrical discharge, which raised the charge on the drops to a level high enough to produce the Taylor cones shown in **Figure 4*c–d***. The almost exact periodicity of the generation process and the steadiness of the charging scheme enabled observation of the evolution of the drops in time by varying the delay Δt between the instant of drop generation and the flash enabling its photograph. These measurements are unique because of the possibility that the shapes observed might correspond to charge levels beyond the Rayleigh limit (at which a pointed drop may be stable).

The best-controlled available images of charged exploding drops with two symmetrically opposed Taylor cones originated in two outstanding reports from Leisner's group (Achtzehn et al. 2005, Duft et al. 2003). Their charged drops are electrodynamically levitated in the presence of relatively weak external fields, and hence approximate the theorist's ideal of being surrounded by a field-free region. In an earlier study (Duft et al. 2002), the authors developed a method based on optical monitoring of externally imposed quadrupole drop oscillations, which are resonant at the Rayleigh limit. Monitoring the amplitude of these oscillations enabled them to show, for the first time, that such drops become unstable exactly at the Rayleigh limit. Earlier reports of anomalous instability below the Rayleigh limit might then be due to changes in the surface tension, following impurity accumulation during drop evaporation. The quadrupole oscillation method also provides a precise means to determine γ right before the instability. In subsequent studies, the monitored amplitude of quadrupolar

oscillation was used to provide an accurate origin of times from which to anticipate the moment of instability. Coupled with an imaging system with a controlled delay, the various phases of the process could be reproducibly recorded with a time resolution of about 5 μs. The sequences published show the initial ellipsoidal elongation of the drop in fine detail, capture an instant of the conical drop with two symmetrically opposed jets, and record the return into a sphere. The time resolution is not sufficient to record several different pointed shapes among the various expected as the drop charge decreases. Two of the photographs presumably obtained at slightly different delay times show an aspect ratio of about 3.7–3.9. Apparently, the process of changing shape is not as fast as that of emitting charge, as hinted by the photographic sequence (the jet lasts less than 5 μs, but the relaxation from a pointed drop back into a sphere takes 60 μs).

5.1. Steady vs Transient Taylor Cones

Due to the scarcity of information on the emissions from charged exploding drops, there have been attempts to extrapolate information obtained from the steady case into the transient case. Fernández de la Mora (1996) argued that the characteristic time for jet formation is much shorter than the duration of the emission; hence, a quasi-steady Taylor cone-jet could form even on a transient Coulombic fission. This point appeared to be confirmed by comparing the charge relaxation time (comparable to the flow time over a characteristic jet radius) to the duration of the transient jet, estimated as the ratio between the charge loss in the fission (known to be between 15% and 50% of q_R) and the emission current (never measured, but taken to be of the order of the minimum current emitted in steady cone-jets). Further confirmation was given by the large ratio of length to width in the jets seen in the Gomez-Tang photo then available, a point now strengthened by the much longer jets of Achtzehn et al. (2005). The provisional conclusion was that the current emission and the daughter drop size were governed by the known laws of steady Taylor cone-jets for highly conducting liquids (fine fission mode), although poor conductors would divide into a few drops of comparable size (rough fission). Li et al. (2005) recently tested this hypothesis by examining the effect of electrical conductivity on daughter drop size. Against the prior assumption of Fernández de la Mora (1996), they argue that the daughter drops from viscous liquids of low conductivity such as triethylene glycol (3EG) must be considerably smaller for the transient than for the steady cone-jets. Independent evidence of radical differences between steady and transient Taylor cones was recently given in numerical computations by Betelú et al. (2006). They consider an infinitely conducting drop charged to the Rayleigh limit at zero Reynolds number (Stokes flow), and follow its evolution in time from an initially slightly nonspherical shape. Within a finite time, the drop develops a doubly conical shape, although with a structure quite different from Taylor's. Instead, the tip evolves in time in a self-similar fashion toward a cone, analogously as in previous studies on the final phases of drop breakup (Blawzdziewicz et al. 1997), where viscous stresses and surface tension balance each other when the surrounding insulator has finite viscosity (Lister & Stone 1998; see also Eggers 1997 for other precedents to these interesting structures). In contrast, surface tension appears to be irrelevant in the self-similar tips of Betelú et al. (2006),

3EG: Triethylene glycol

who state that the balance is between viscous and electrical stresses. Furthermore, the cone angle depends on the ratio of viscosities, and is in all cases considerably smaller than Taylor's. This geometrical feature is in qualitative agreement with the photographs shown in **Figures 1*b*** and **4*b*** for transient drops. The computed aspect ratio of about 4 agrees quantitatively with **Figure 1*b***, but not with **Figure 4*b***. The differences are probably due to large variations in the physical properties of heptane and EG. For instance, the Reynolds number $\mathrm{Re} = (\rho\gamma R)^{1/2}/\mu$ is large for heptane, but of order one for EG. The characteristic time for shape change is much shorter in heptane [$t_p \sim (\rho R^3/\gamma)^{1/2}$ at high Re] than in EG ($t_p \sim R\mu/\gamma$ at small Re). The electrical conductivity K of the heptane drop of **Figure 4** is fairly small, with an electrical relaxation time $\tau_e = \varepsilon\varepsilon_o/K$ of about 17 μs, whereby the jet ejection time is probably large compared with t_p. This point is confirmed for another low-viscosity liquid (acetone) in the photographs of Hager et al. (1994) (**Figure 4*d***), where the jet lasts for relatively long periods, over which the drop shape varies drastically. Hence, there is enough time to achieve a hydrostatic equilibrium shape in low viscosity liquids such as heptane and acetone, but not in EG, and even less in the liquid (3EG) studied by Li et al. (2005). For this reason, the emission of daughter droplets in fissions of viscous drops is likely influenced by the transient non-Taylor equilibrium shape of Betelú et al. (2006), whose associated jet is bound to differ from Taylor cone-jets, as first hinted by Li et al. (2005).

Note that the fact that the angles observed in both heptane and EG are closer to those of Betelú et al. (2006) than to Taylor's is insufficient to cast aside a balance between surface tension and electrical stresses. This can be rationalized in various ways (one of them based on space charge effects associated with the jet; see Section 4.2). For instance, Coulombic fissions driven not by net charge but by an external field (**Figure 1*d***) also show cone angles substantially smaller than Taylor's, yet a quasi-steady state can certainly be reached because the emission of charge is bipolar, the drop remains neutral at all times, and the jet lifetime may be substantial.

6. SMALLEST POSSIBLE JET, ION EVAPORATION, AND THE PURELY IONIC REGIME

At a fixed electrical conductivity K there is a minimum flow rate at which the smallest possible drops and jets are produced. This smallest attainable size decreases with increasing K, but the scaling laws discussed in Section 4.6 are not valid at arbitrarily large conductivities. When $K \sim 1$ S/m, the maximum electric field E_{max} on the meniscus surface reaches values of the order of 1 V/nm, at which point ions begin to escape from the liquid into the gas (Iribarne & Thomson 1976, Loscertales & Fernández de la Mora 1995, Thomson & Iribarne 1979), with ion current levels I_i that grow rapidly with E_{max} and soon become dominant (Gamero-Castaño & Fernández de la Mora 2000). The possibilities of a purely ionic regime and a mixed regime of simultaneous ion and drop ejection are well known in Taylor cones of liquid metals (Gabovich 1984, Prewett & Mair 1991). In this case, K is many orders of magnitude larger than in electrolytes, charge relaxation phenomena are nonexistent, and the electric field cannot be controlled externally. Ion production from Taylor cones of electrolytes of

several low volatility substances (mostly glycerol) held in a vacuum has been studied primarily for mass spectrometry (Cook 1986), although the phenomenon also takes place in so-called colloidal propulsion (Perel et al. 1969). The appearance of small ion currents, and even conditions in which ions carry more than 90% of the total current, have been observed at high conductivities (~1 S/m) and low flow rates (Gamero-Castaño & Fernández de la Mora 2000; Gamero-Castaño & Hruby 2001, 2002; Guerrero et al. 2006), but drops have also been seen in electrolytes (formed by mixtures of salts and neutral solvents), showing that a jet is still present. However, in a few molten salts, purely ionic emission has been observed (Chiu et al. 2005, Lozano 2006, Lozano & Martinez-Sánchez 2005, Romero-Sanz et al. 2003, Romero-Sanz & Fernández de la Mora 2004), revealing a transition between an open cone-jet and the closed meniscus geometry typical of liquid metals. The reasons why some molten salts exhibit the purely ionic regime (presumably without a jet), whereas others do not, remain unclear. It seems, however, that the combination of a high electrical conductivity and a high surface tension helps to suppress the drops (Martino et al. 2006). Ion evaporation drastically changes the behavior of Taylor cones, and very little is theoretically known about the mixed ion-drop regime or the purely ionic regime. Some features from the liquid metal literature will nonetheless be useful to resolve these difficulties (Higuera 2004).

SUMMARY POINTS

1. A hydrostatic section extends Taylor's work to curved interfaces and discusses available evidence for hysteretic phenomena.
2. Saville's extended leaky dielectric model is used to illustrate the limitations of the ohmic conduction model and to show the creation of traveling fronts of charge-depleted regions near the free surface.
3. The scaling laws for the jet shape and the emitted current are reviewed together with the reasons for the lack of electrostatic parameter influence.
4. The similarities and differences between steady cone-jets and the transient jets forming in charged exploding drops are noted.
5. The special features associated with ion evaporation arising at high electrical conductivity are discussed, including a recently discovered purely ionic regime in molten salts, where the jet disappears and only ions are emitted from the tip.

FUTURE ISSUES

1. What determines the minimum flow rate in a steady Taylor cone-jet?
2. Does the electrostatic limit ever describe the bulk of the shape of an exploding drop?

3. How does the structure of the transient jet formed on a Coulombic fission differ from its steady cone-jet analog?
4. What determines the structure of ion-emitting Taylor cones in the mixed (ion + drop) regime and in the purely ionic regime?

ACKNOWLEDGMENTS

I am indebted to Professors Francisco Higuera (Madrid) and Manuel Martinez-Sanchez (Boston) for many improvements on the manuscript. This work has been supported by U.S. AFOSR grants F49620-01-1-0416 and FA9550-06-1-104, and by two AFOSR subcontracts from the companies Busek and Connecticut Analytical.

LITERATURE CITED

Achtzehn T, Müller R, Duft D, Leisner T. 2005. The Coulomb instability of charged microdroplets: dynamics and scaling. *Eur. Phys. J. D* 34:311–13

Barrero A, Gañán-Calvo AM, Dávila J, Palacio A, Gómez-Gonzále E. 1998. Low and high Reynolds number flows inside Taylor cones. *Phys. Rev. E* 58:7309–14

Barrero A, López-Herrera JM, Boucard A, Loscertales IG, Marquez M. 2004. Steady cone-jet electrosprays in liquid insulator baths. *J. Colloid Interface Sci*. 272:104–8

Betelú SI, Fontelos MA, Kindelán U, Vantzos O. 2006. Singularities on charged viscous droplets. *Phys. Fluids* 18:051706

Blawzdziewicz J, Cristini V, Loewenberg M. 1997. Analysis of drop breakup in creeping flow. *Bull. Am. Phys. Soc*. 42(11):2125

Brazier-Smith PR, Jennings S, Latham J. 1971. An investigation on the behavior of drops and drop pairs subjected to strong electrical forces. *Proc. R. Soc. London Ser.* A 325:363–76

Carretero-Benignos JA. 2005. *Numerical simulation of a single emitter colloid thruster in pure droplet cone-jet mode*. Ph.D. thesis. Mass. Inst. Technol. **http://ssl.mit.edu/publications/theses/PhD-2005-Carretero-BenignosJorge.htm**

Chen DR, Pui DYH. 1997. Experimental investigation of scaling laws for electrospraying: Dielectric constant effect. *Aerosol. Sci. Technol*. 27:367–80

Cherney L. 1999. Structure of Taylor cone-jets: limit of low flow rates. *J. Fluid Mech*. 378:167–96

Chiu YH, Austin BL, Dressler RA, Levandier D, Murray PT, et al. 2005. Mass spectrometric analysis of colloid thruster ion emission from selected propellants. *J. Propuls. Power* 21:416–23

Cloupeau M. 1994. Recipes for use of EHD spraying in cone-jet mode and notes on corona discharge. *J. Aerosol Sci*. 25:1143–57

Cloupeau M, Prunet-Foch B. 1989. Electrostatic spraying of liquids in cone-jet mode. *J. Electrost*. 22:135–59

Cloupeau M, Prunet-Foch B. 1990. Electrostatic spraying of liquids. Main functioning modes. *J. Electrost*. 25:165–84

Cloupeau M, Prunet-Foch B. 1994. Electrohydrodynamic spraying functioning modes: a critical review. *J. Aerosol Sci*. 25:1021–36
Cook KD. 1986. Electrohydrodynamic mass-spectrometry. *Mass Spectrom. Rev*. 5:467–519
de Juan L, Fernández de la Mora J. 1997. Charge and size distributions of electrospray drops. *J. Colloid Interface Sci*. 186:280–93
Duft D, Achtzehn T, Müller R, Huber BA, Leisner T. 2003. Coulomb fission: Rayleigh jets from levitated microdroplets. *Nature* 421:128
Duft D, Lebius H, Huber BA, Guet C, Leisner T. 2002. Shape oscillations and stability of charged microdroplets. *Phys. Rev. Lett*. 89:084503
Eggers J. 1997. Nonlinear dynamics and breakup of free-surface flows. *Rev. Mod. Phys*. 69:865–929
Fenn JB. 1996. Research in retrospect: Some Biograffiti of a Journeyman Chemist. *Annu. Rev. Phys. Chem*. 47:1–41
Fenn JB, Mann M, Meng CK, Wong SK, Whitehouse CM. 1989. Electrospray ionisation for mass spectrometry of large biomolecules. *Science* 246:64–71
Fernández de la Mora J. 1992. The effect of charge emission from electrified liquid cones. *J. Fluid Mech*. 243:561–74
Fernández de la Mora J. 1996. On the outcome of the Coulombic fission of a charged isolated drop. *J. Colloid Interface Sci*. 178:209–18
Fernández de la Mora J, Loscertales IG. 1994. The current transmitted through an electrified conical meniscus. *J. Fluid Mech*. 260:155–84
Gabovich MD. 1984. Liquid-metal emitters. *Sov. Phys. Usp*. 26:447–55
Gamero-Castaño M, Fernández de la Mora J. 2000. Direct measurement of ion evaporation kinetics from electrified liquid surfaces. *J. Chem. Phys*. 113:815–32
Gamero-Castaño M, Hruby V. 2001. Electrospray as a source of nanoparticles for efficient colloid thrusters. *J. Propuls. Power* 17:977–87
Gamero-Castaño M, Hruby V. 2002. Electric measurements of charged sprays emitted by cone-jets. *J. Fluid Mech*. 459:245–76
Gañán-Calvo AM. 1997. Cone-jet analytical extension of Taylor's electrostatic solution and the asymptotic universal scaling laws in electrospraying. *Phys. Rev. Lett*. 79:217
Gañán-Calvo AM. 1999. The surface charge in electrostatic spraying: its nature and its universal Scaling laws. *J. Aerosol Sci*. 30:863–72
Gañán-Calvo AM. 2004. On the general scaling theory for electrospraying. *J. Fluid Mech*. 507:203–12
Gañán-Calvo AM, Dávila J, Barrero A. 1997. Curent and droplet size in the electrospraying of liquids. Scaling laws. *J. Aerosol Sci*. 28:249–75
Gañán-Calvo AM, Lasheras JC, Dávila J, Barrero A. 1994. The electrostatic spray emitted from an electrified conical meniscus. *J. Aerosol Sci*. 25:1121–42
Gomez A, Tang K. 1994. Charge and fission of droplets in electrostatic sprays. *Phys. Fluids* 6:404–14
Grimm RL, Beauchamp JL. 2005. Dynamics of field-induced droplet ionization: Time-resolved studies of distortion, jetting, and progeny formation from charged and neutral methanol droplets exposed to strong electric fields. *J. Phys. Chem. B* 109:8244–50

Ha J-W, Yang S-M. 2000. Deformation and breakup of Newtonian and non-Newtonian conducting drops in an electric field. *J. Fluid Mech*. 405:131–56

Hager DB, Dovichi NJ. 1994. Behaviour of microscopic liquid droplets near a strong electrostatic field: droplet electrospray. *Anal. Chem*. 66:1593–94

Hager DB, Dovichi NJ, Klassen J, Kebarle P. 1994. Droplet electrospray mass spectrometry. *Anal. Chem*. 66:3944–49

Hayati I, Bailey AI, Tadros TF. 1986. Mechanism of stable jet formation in electrohydrodynamic atomization. *Nature* 319:41–43

Higuera FJ. 2004. Liquid flow induced by ion evaporation in an electrified meniscus. *Phys. Rev. E* 69:066301

Higuera FJ. 2003. Flow rate and electric current emitted by a Taylor cone. *J. Fluid Mech*. 484:303–27

Hohman MM, Shin M, Rutledge G, Brenner MP. 2001a. Electrospinning and electrically forced jets. I. Stability theory. *Phys. Fluids* 13:2201–20

Hohman MM, Shin M, Rutledge G, Brenner MP. 2001b. Electrospinning and electrically forced jets. II. Applications. *Phys. Fluids* 13:2221–36

Iribarne JV, Thomson BA. 1976. On the evaporation of small ions from charged droplets. *J. Chem. Phys*. 64:2287–94

Landau LD, Lifshitz EM. 1960. *Electrodynamics of Continuous Media*, Chapter 1, Problem 6. Oxford, UK: Pergamon

Li KY, Tu H, Ray AK. 2005. Charge limits on droplets during evaporation. *Langmuir* 21:3786–94

Lister JR, Stone HA. 1998. Capillary breakup of a viscous thread surrounded by another viscous fluid. *Phys. Fluids* 10:2758–64

López-Herrera JM, Riesco-Chueca P, Gañán-Calvo AM. 2005. Linear stability analysis of axisymmetric perturbations in imperfectly conducting liquid jets. *Phys. Fluids* 17:034106

Loscertales IG, Fernández de la Mora J. 1995. Experiments on the kinetics of field evaporation of small ions from droplets. *J. Chem. Phys*. 103:5041–60

Lozano P, Martínez-Sánchez M. 2005. Ionic liquid ion sources: characterization of externally wetted emitters. *J. Colloid Interface Sci*. 282:415–21

Lozano P. 2006. Energy properties of an EMI-Im ionic liquid ion source. *J. Phys. D. Appl. Phys*. 39:126–34

Martino W, Fernández de la Mora J, Yoshida Y, Saito G, Wilkes J. 2006. Surface tension measurements of highly conducting ionic liquids. *Green Chem*. 8:390–97

Melcher JR, Taylor GI. 1969. Electrohydrodynamics: a review of the role of interfacial shear stresses. *Annu. Rev. Fluid Mech*. 1:111–46

Michelson D. 1990. *Electrostatic Atomization*. Bristol: Hilger

Pantano C, Gañán-Calvo AM, Barrero A. 1994. Zeroth-order, electrohydrostatic solution for electrospraying in cone-jet mode. *J. Aerosol Sci*. 25:1065–77

Perel J, Mahoney JF, Moore RD, Yahiku AY. 1969. Research and development of a charged-particle bipolar thruster. *AIAA J*. **7**:507

Prewett PD, Mair GLR. 1991. *Focused Ion Beams from Liquid Metal Ion Sources*. Taunton, UK: Res. Stud. Press Wiley

Ramos A, Castellanos A. 1994. Conical points in liquid-liquid interfaces subjected to electric fields. *Phys. Lett. A* 184:268–72
Rayleigh L. 1882. On the equilibrium of conducting masses charged with electricity. *Philos. Mag*. 14:184–86
Rayleigh L. 1945. *The Theory of Sound*. New York: Dover
Reznik SN, Yarin AL, Theri A, Zussman E. 2004. Transient and steady shapes of droplets attached to a surface in a strong electric field. *J. Fluid Mech*. 516:349–77
Richardson CB, Pigg AL, Hightower RL. 1989. On the stability limit of charged droplets. *Proc. R. Soc. London Ser. A* 422:319–28
Romero-Sanz I, Bocanegra R, Fernández de la Mora J, Gamero-Castaño M. 2003. Source of heavy molecular ions based on Taylor cones of ionic liquids operating in the pure ion evaporation regime. *J. Appl. Phys*. 94:3599–605
Romero-Sanz I, Fernández de la Mora J. 2004. Spatial structure and energy distribution of electrosprays of ionic liquids in vacuo. *J. Appl. Phys*. 95:2123–29
Rosell J, Fernández de la Mora J. 1994. Generation of monodisperse droplets 0.3 to 4 μm in diameter from electrified cone-jets of highly conducting viscous liquids. *J. Aerosol Sci*. 25:1093–1119
Saville DA. 1997. Electrohydrodynamics: The Taylor-Melcher Leaky Dielectric Model. *Annu. Rev. Fluid Mech*. 29:27–64
Smith DPH. 1986. The electrohydrodynamic atomization of liquids. *IEEE Trans. Ind. Appl.* IA-22:527–35
Smith KL, Alexander MS, Stark JPW. 2006. Voltage effects on the volumetric flow rate in cone-jet mode electrospraying. *J. Appl. Phys.* 99:064909
Stone HA, Lister JR, Brenner MP. 1999. Drops with conical ends in electric and magnetic fields. *Proc. R. Soc. London Ser. A* 455:329–47
Tang K, Gomez A. 1994a. On the structure of an electrostatic spray of monodisperse droplets. *Phys. Fluids* 6:2317–22
Tang K, Gomez A. 1994b. Generation by electrospray of monodisperse water droplets for targeted drug delivery by inhalation. *J. Aerosol Sci.* 25:1237–49
Tang K, Gomez A. 1995. Generation of monodisperse water droplets from electrosprays in a corona-assisted cone-jet mode. *J. Colloid Interface Sci*. 175:326–32
Tang KQ, Gomez A. 1996. Monodisperse electrosprays of low electric conductivity liquids in the cone-jet mode. *J. Colloid Interface Sci*. 184:500–11
Taylor GI. 1964. Disintegration of water drops in an electric field. *Proc. R. Soc. London Ser. A* 280:383–97
Taylor GI. 1965. The stability of a horizontal fluid interface in a vertical electric field. *J. Fluid Mech*. 2:1–15
Taylor GI. 1966. Studies in electrohydrodynamics. I. The circulation produced in a drop by an electric field. *Proc. R. Soc. London Ser. A* 291:159–66
Thomson BA, Iribarne JV. 1979. Field induced ion evaporation from liquid surfaces at atmospheric pressure. *J. Chem. Phys*. 71:4451–63
Zeleny J. 1915. On the conditions of instability of liquid drops, with applications to the electrical discharge from liquid points. *Proc. Camb. Philos. Soc*. 18:71–93
Zeleny J. 1917. Instability of electrified liquid surfaces. *Phys. Rev*. 10:1–6
Zeleny J. 1935. The role of surface instability in electrical discharges from drops of alcohol and water in air at atmospheric pressure. *J. Franklin Inst*. 219:659–75

Annual Review of
Fluid Mechanics

Volume 39, 2007

Contents

Indexes

Errata

An online log of corrections to *Annual Review of Fluid Mechanics* chapters (1997 to the present) may be found at http://fluid.annualreviews.org/errata.shtml